Journal of Experimental Botany, Vol. 66, No. 5 pp. 1303–1315, 2015
doi:10.1093/jxb/eru481 Advance Access publication 29 December 2014
This paper is available online free of all access charges (see http://jxb.oxfordjournals.org/open_access.html for further details)

RESEARCH PAPER

Increasing leaf hydraulic conductance with transpiration rate minimizes the water potential drawdown from stem to leaf

Kevin A. Simonin[1,*], Emily Burns[2], Brendan Choat[3], Margaret M. Barbour[4], Todd E. Dawson[5] and Peter J. Franks[4]

[1] Department of Biology, San Francisco State University, San Francisco, CA 94132, USA
[2] Save The Redwoods League, 111 Sutter Street, 11th Floor, San Francisco, CA 94104, USA
[3] University of Western Sydney, Hawkesbury Institute for the Environment, Locked Bag 1797, Penrith 2751, NSW, Australia
[4] Faculty of Agriculture and Environment, University of Sydney, NSW 2006, Australia
[5] Department of Integrative Biology, University of California-Berkeley, Berkeley, CA 94720, USA

* To whom correspondence should be addressed. E-mail: simonin@sfsu.edu

Received 11 July 2014; Revised 3 November 2014; Accepted 4 November 2014

Abstract

Leaf hydraulic conductance (k_{leaf}) is a central element in the regulation of leaf water balance but the properties of k_{leaf} remain uncertain. Here, the evidence for the following two models for k_{leaf} in well-hydrated plants is evaluated: (i) k_{leaf} is constant or (ii) k_{leaf} increases as transpiration rate (*E*) increases. The difference between stem and leaf water potential ($\Delta\Psi_{stem-leaf}$), stomatal conductance (g_s), k_{leaf}, and *E* over a diurnal cycle for three angiosperm and gymnosperm tree species growing in a common garden, and for *Helianthus annuus* plants grown under sub-ambient, ambient, and elevated atmospheric CO_2 concentration were evaluated. Results show that for well-watered plants k_{leaf} is positively dependent on *E*. Here, this property is termed the dynamic conductance, $k_{leaf(E)}$, which incorporates the inherent k_{leaf} at zero *E*, which is distinguished as the static conductance, $k_{leaf(0)}$. Growth under different CO_2 concentrations maintained the same relationship between k_{leaf} and *E*, resulting in similar $k_{leaf(0)}$, while operating along different regions of the curve owing to the influence of CO_2 on g_s. The positive relationship between k_{leaf} and *E* minimized variation in $\Delta\Psi_{stem-leaf}$. This enables leaves to minimize variation in Ψ_{leaf} and maximize g_s and CO_2 assimilation rate over the diurnal course of evaporative demand.

Key words: Leaf hydraulic conductance, leaf water potential, stem water potential, stomatal conductance, transpiration, water relations.

Introduction

The co-variation between leaf water potential (Ψ_{leaf}), transpiration rate (*E*), stomatal conductance (g_s), and CO_2 assimilation rate (*A*) at any instant in time, or integrated over the life of a leaf, is considered to be strongly influenced by the water permeability of the cells that define the leaf hydraulic network (e.g. Sôber, 1997; Franks, 2006; Sack and Holbrook, 2006; Brodribb *et al.*, 2007; Simonin *et al.*, 2012). The cell types that comprise the leaf hydraulic network vary greatly in structure and function. At one extreme are the relatively rigid, dead, xylem cells comprising solely of cell wall, and at the other extreme are the live parenchyma cells of the extra-xylary tissue. At the whole-leaf level these two cell types in combination represent, on average, ~50% of the total liquid-phase conductance to water flow along the transpiration stream between the roots and sites of evaporation within the leaves of a plant (Nardini *et al.*, 2005*a*; Sack *et al.*, 2005). Thus, in response to variation in water availability or demand, the conductance of both the leaf xylem and extra-xylary pathways strongly influence the changes in liquid flux.

Models used to describe changes in leaf hydraulic conductance (k_{leaf}), in response to variation in water availability or demand, are often based on dynamics previously observed in stems by emphasizing xylem vulnerability to cavitation as Ψ_{leaf} decreases (e.g. Brodribb and Holbrook, 2006). According to this xylem-centric framework, k_{leaf} is at a maximum when leaves are well hydrated (i.e. high Ψ_{leaf}). As E increases, k_{leaf} may stay relatively constant, with Ψ_{leaf} decreasing until a threshold is reached that results in the formation of xylem emboli, followed by a rapid decline in k_{leaf} with any further decrease in Ψ_{leaf} (e.g. Blackman *et al.*, 2009; Johnson *et al.*, 2009; Martorell *et al.*, 2014). Under this scenario, increases in E would increase the driving gradient for water flow across a leaf. In other words, above the cavitation threshold a positive linear relationship is expected between the water potential difference between stem and leaf ($\Delta\Psi_{stem–leaf}$) and E (e.g. Fig. 1, solid black line).

Xylem-focused models have been extremely useful for characterizing the extent to which emboli induced by water stress begin to limit leaf gas exchange and primary productivity (e.g. Salleo *et al.*, 2001; Sperry *et al.*, 2002; Cochard *et al.*, 2002; Johnson *et al.*, 2012). However, it is becoming increasingly apparent that changes in how water is transported through the extra-xylary component of the transpiration stream can lead to large, sustained changes in k_{leaf} before or even after the onset of cavitation (e.g. Matzner and Comstock, 2001; Lo Gullo *et al.*, 2005; Nardini *et al.*, 2005*b*; Cochard *et al.*, 2007; Sellin and Kupper, 2007; Sellin *et al.*, 2008; Scoffoni *et al.*, 2008; Pou *et al.*, 2013; Shatil-Cohen *et al.*, 2011). These observations suggest an additional mechanism driving the co-variation between Ψ_{leaf}, E, g_s, and k_{leaf} that cannot be explained by models that emphasize xylem vulnerability to cavitation. As the vast majority of carbon gain and water use occurs when leaf water potentials are above the water potential thresholds that lead to significant loss of hydraulic conductance via xylem embolism, there is a need for a greater understanding of the mechanisms governing the co-variation between Ψ_{leaf}, E, g_s, k_{leaf}, and ultimately A when leaves are well hydrated. A comprehensive quantification of the relationship between k_{leaf}, g_s, and E is crucial in vegetation models that incorporate hydraulic processes.

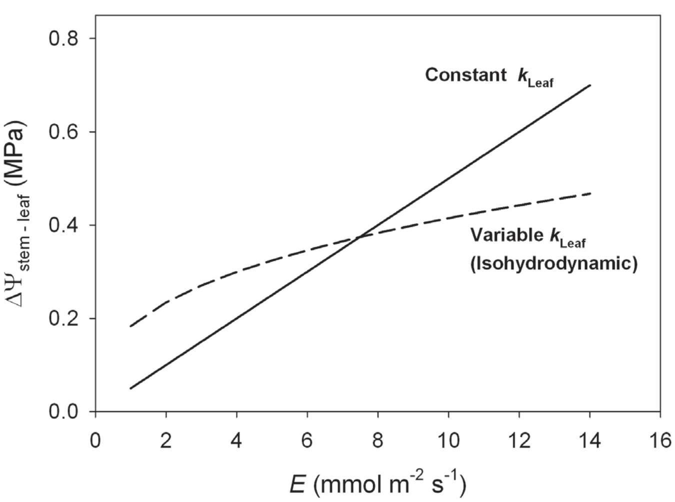

Fig. 1. Two models describing the water potential drawdown from stem to leaf ($\Delta\Psi_{stem–leaf}$, MPa) in response to changes in transpiration rate (E, mmol m^{-2} s^{-1}). The solid black line represents a model scenario when leaf hydraulic conductance (k_{leaf}, mmol m^{-2} s^{-1} MPa^{-1}) is constant, whereas the dashed line represents a model scenario when k_{leaf} is positively dependent on E, commonly referred to as isohydrodynamic conditions.

Although stomata and the leaf hydraulic network control two distinct phases of water transport across the soil–plant–atmosphere continuum (i.e. vapour and liquid flux), coordination between these two regulatory systems must exist if leaves are to maintain physiologically favourable water contents and avoid desiccation while maximizing carbon gain. If the goal is to maximize carbon gain, then leaves need to keep stomata open over a broad diurnal range of evaporative demand. The problem for any leaf with fixed k_{leaf}, or one in which k_{leaf} only declines with increasing E, is that the water potential drawdown ($\Delta\Psi_{stem–leaf}$) increases with E which, via the hydraulic feedback loop, tends to reduce g_s and CO_2 assimilation rate (Cowan, 1977; Buckley, 2005; Franks *et al.*, 2007). One solution to this problem is for leaves to vary k_{leaf} positively with E to minimize the change in $\Delta\Psi_{stem–leaf}$, maintaining isohydrodynamic conditions. Leaves operating with this mechanism will show a nonlinear relationship between $\Delta\Psi_{stem–leaf}$ and E where the ratio of E to $\Delta\Psi_{stem–leaf}$ increases as E increases (Fig. 1, dashed line). In other words, a positive correlation between k_{leaf} and E would reduce daytime depressions in Ψ_{leaf} and increase the maximum potential g_s and A for a given leaf to air vapour pressure difference (VPD).

Isohydrodynamic behaviour has been shown for whole-plant hydraulic conductance (Franks *et al.*, 2007). Reports of relatively constant $\Delta\Psi_{stem–leaf}$ (Black, 1979; Brodribb and Holbrook, 2003) suggest that the same mechanism may operate at the leaf level. Here the hypothesis that variation in g_s and k_{leaf} are connected through optimization of the water potential drawdown across a leaf is tested. Specifically, it is predicted that variation in k_{leaf} occurs to maximize leaf gas exchange while minimizing variation in $\Delta\Psi_{stem–leaf}$. Using *in situ* measurements of k_{leaf} taken on species grown under well-watered conditions in a common garden and on plants grown under three different atmospheric CO_2 concentrations, two possible models describing the mechanistic links between Ψ_{leaf}, E, g_s, and k_{leaf} in well-hydrated plants are tested: (i) constant k_{leaf}, versus (ii) increasing k_{leaf} as E increases.

Materials and methods

Common garden

Four deciduous and two evergreen temperate forest tree species were evaluated; three angiosperms, *Acer macrophyllum* Pursh (Aceraceae), *Populus fremontii* Watson (Salicaceae), and *Quercus kelloggii* Newberry (Fagaceae), and three gymnosperms, *Metasequoia glyptosrtoboides* Hu and Cheng (Cupressaceae), *Pinus ponderosa* P. Laws (Pinaceae), and *Sequoia sempervirens* D. Don (Cupressaceae). Four or five saplings of each species were grown from seed in 40 l pots and transferred to a single site (common garden), in full sun, on a ridge top at the University of California Botanical Garden (32°52´N 122°14´W, ~256 m elevation) between 1–7 March 2007. Individual saplings from each species were randomized spatially throughout the common garden. Saplings ranged from ~1.5–2.5 m in height. Plants were kept well watered using drip irrigation. Data were collected when leaves were fully expanded, ~1 month after the start of leaf emergence, which occurred in late May/early June of 2008 and 2009 for *A. macrophyllum*, *M. glyptostroboides*, *P. fremontii*, and *Q. kelloggii* and mid to late July for *P. ponderosa*, and *S. sempervirens*. Air temperature and relative humidity were measured with a Li-1600 steady-state porometer (Licor Inc., Lincoln NE, USA) in close proximity to the leaves in which gas exchange and water potential were measured. Photosynthetically active radiation intercepted by the adaxial surface of the leaf was measured with a quantum sensor (Model Li-190SB, Licor Inc., Lincoln NE, USA).

Diurnal variation in leaf hydraulic conductance (k_{leaf}; mmol m^{-2} s^{-1} MPa^{-1}) for sun-exposed leaves was measured on four to five individuals of each species using the *in* situ evaporative flux method (*in situ* EFM), with k_{leaf} calculated as (Brodribb and Holbrook, 2003):

$$k_{leaf} = E/\Delta\Psi_{stem\text{-}leaf} \quad (1)$$

where E is the transpiration rate (mmol m^{-2} s^{-1}), and $\Delta\Psi_{stem-leaf}$ is the difference between stem xylem water potential (Ψ_{stem}; MPa) and leaf water potential (Ψ_{leaf}; MPa). This *in situ* technique required sampling two adjacent leaves, one of which was used to measure Ψ_{stem} whereas the adjacent leaf was sampled for E and Ψ_{leaf}. Leaves used as an assay for Ψ_{stem} were covered in plastic film and aluminium foil on the evening before the measurement period to ensure equilibration between the covered Ψ_{leaf} and Ψ_{stem}. Transpiration rate (E) was measured with the Li-1600 porometer. Owing to the open crown structure of the saplings, the wide spacing between trees, and the windy ridge top exposure of the common garden, it was assumed that leaf boundary layer conductance (g_b) was much greater than g_s. Additionally, during each measurement of E, leaf orientation, ambient humidity, and radiation interception was conserved. Therefore, E measured by the Li-1600 was likely to be similar to the actual E immediately before the measurement. While measuring E, the water potential of the adjacent covered leaf was sampled as a proxy for Ψ_{stem}. Immediately following determination of E, the uncovered leaf was excised, wrapped in plastic, and placed in a Scholander-type pressure chamber for determination of Ψ_{leaf} (Soil Moisture Equipment Corp., Santa Barbara CA, USA). Balancing pressure was recorded when xylem sap reached the cut stem surface, as verified by a dissecting scope at ×25 magnification. E, Ψ_{stem}, and Ψ_{leaf} were measured every ~2.5 h over the course of a 14–18 h period, beginning at pre-dawn (0400–0500 h). Regression analysis was used to evaluate the co-variation between $\Delta\Psi_{stem-leaf}$, E, g_s, and k_{leaf} over a diurnal cycle of evaporative demand. Regression analyses were performed using SigmaPlot (Version 11; Systat Software Inc., San Jose, CA, USA).

Growth chamber experiment

$\Delta\Psi_{stem-leaf}$, E, g_s, A, and k_{leaf} were measured at two light levels (509 ± 11.5 and 1310 ± 26.4 μmol m^{-2} s^{-1}) for *Helianthus annuus* plants grown under sub-ambient (194 ± 35 ppm), ambient (450 ± 46 ppm), and elevated CO_2 (1027 ± 74 ppm). *H. annuus* plants were grown in growth chambers located in the Controlled Environment Facility at the Center for Carbon, Water, and Food at the University of Sydney. Ten plants were grown under each CO_2 concentration at 900 ± 50 μmol m^{-2} s^{-1} of photosynthetically active radiation (PAR). Ambient CO_2 concentrations were monitored using an isotope ratio infrared spectrometer (G1101-i, Picarro, CA, USA) that cycled through each room every 10 min. Using the method outlined above, g_s and E were measured with a portable photosynthesis system fitted with a large leaf cuvette that enclosed the entire leaf (Walz-USA, Pepperell MA, USA). Water potential was measured using a Scholander-style pressure chamber (Soil Moisture Equipment Co., Santa Barbara CA, USA) and k_{leaf} was calculated from Eqn 1. Measurements were taken after the leaves were in the cuvette for ~40 min during stable g_s, E, A, and T_{leaf}. After the 40 min period leaves were cut from the stem, removed from the cuvette, and covered in plastic for water potential measurements with the Scholander-style pressure chamber as described above. Projected leaf area was measured digitally using the software program Image J (US National Institutes of Health, Bethesda, Md). Two leaves were used as an assay for Ψ_{stem} using the method outlined above. Leaves directly above and below the leaf in the cuvette were selected and the average of the two water potential measurements was taken as Ψ_{stem}. In all cases the distal leaf showed a slightly more negative Ψ_{stem}, ~0.02–0.04 MPa. Measurements of Ψ_{leaf}, E, g_s, A, and k_{leaf} were made at 450 ppm CO_2 inside the cuvette at two light levels, ~500 and 1300 μmol m^{-2} s^{-1} PAR, and a relatively constant leaf temperature of 24.7 ± 0.2 °C by varying air temperature and ambient humidity inside the cuvette. In total, five leaves from each CO_2 growth environment were measured at each light level (~500 and 1300 μmol m^{-2} s^{-1} PAR), all at 450 ppm CO_2. All statistical analyses were performed using SigmaPlot and JMP (v.4.0.4; SAS Institute, Cary, NC, USA). ANCOVA was used to test for main and interactive effects of growth CO_2 (low, medium, and high), light (low, high), and VPD on g_s and A. An ANCOVA was also used to test for main and interactive effects of CO_2 (low, medium and high), light (low, high), and E (covariate) on k_{leaf}. Because measurements within the light treatment were done on the same plant, plants nested within the light treatment were used as a random factor (Quinn and Keough, 2002). Assumptions of normality were met.

Estimation of k_{leaf} when E=0

As shown by Eqn 1, using the *in situ* EFM technique to measure k_{leaf} requires an evaporative flux and a water potential drawdown which in turn prevents direct calculation of k_{leaf} when E=0. However, theory predicts that when E=0, k_{leaf} will have some finite value. By measuring k_{leaf} across a broad range of E a linear model can be used to extrapolate to k_{leaf} at zero E (i.e. the static conductance, $k_{leaf(0)}$). Linear regression was used to estimate $k_{leaf(0)}$ for both gymnosperm and angiosperm trees from the common garden and *H. annuus* plants from the growth chamber experiment.

Results

Common garden

A strong non-linear relationship was observed between $\Delta\Psi_{stem-leaf}$ and E for both the gymnosperm (Fig. 2) and angiosperm species (Fig. 3) from the common garden. Although the maximum transpiration rates for the gymnosperm species were lower than the angiosperm species (Table 1), on average, the co-variation between $\Delta\Psi_{stem-leaf}$ and E was similar between species (gymnosperms, $y=0.18x^{0.35}$, $r^2=0.44$, $P<0.001$; angiosperms, $y=0.14x^{0.48}$, $r^2=0.69$, $P<0.001$), with angiosperms attaining higher overall $\Delta\Psi_{stem-leaf}$ and E (Fig. 4). Assuming liquid fluxes into the leaf and vapour phase fluxes from the leaf were in steady-state, the observed correlation between $\Psi_{stem-leaf}$ and E was the result of a strong coupling between k_{leaf} and E (Table 1). A significant positive relationship was observed between k_{leaf} and E across the gymnosperm and angiosperm species from the common garden (Figs 2, 3, 5). For each species the y-intercept of the linear model describing the co-variation between k_{leaf} and E was greater than 0 (Figs 2, 3; Table 1). This static leaf hydraulic conductance when E=0 ($k_{leaf(0)}$), varied greatly between angiosperm and gymnosperm species (Figs 2, 3; Table 1), with angiosperms having a higher $k_{leaf(0)}$ (Fig. 5; Table 1). For the plants growing in the common garden, a higher $k_{leaf(0)}$ was associated with greater maximum daytime g_s, k_{leaf}, and lower dk_{leaf}/dE (Fig. 6;

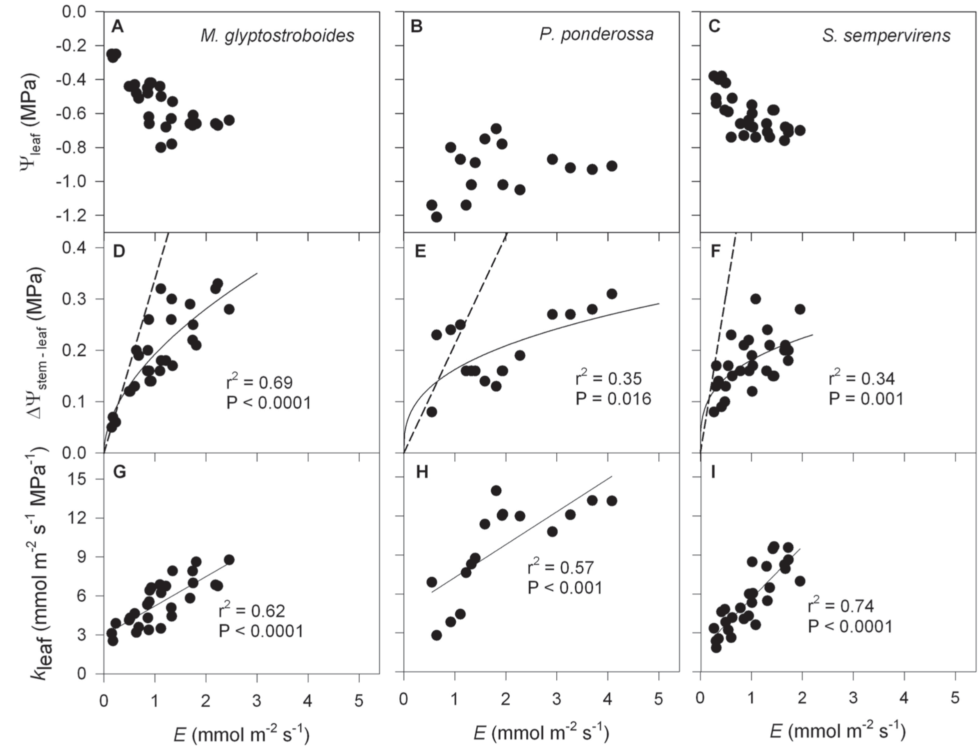

Fig. 2. Variation in leaf water potential (Ψ_{leaf}, MPa), the difference between stem and leaf water potential ($\Delta\Psi_{stem–leaf}$, MPa), and leaf hydraulic conductance (k_{leaf}, mmol m^{-2} s^{-1} MPa^{-1}) as a function of transpiration rate (E, mmol m^{-2} s^{-1}) for the three gymnosperm species from the common garden: *M. glyptostroboides* (A, D, G); *P. ponderosa* (B, E, H); and *S. sempervirens* (C, F, I). The solid black line in each panel represent the best-fit model describing the coordination between $\Psi_{stem–leaf}$ and k_{leaf} with variation in E. The dashed lines in panels D, E, and F represent the predicted changes in $\Delta\Psi_{stem–leaf}$ for a leaf that possesses the average static leaf hydraulic conductance (i.e. $k_{leaf(0)}$) for each individual species. The coefficient of determination (r^2) and significance (P) in each panel refer to the solid lines.

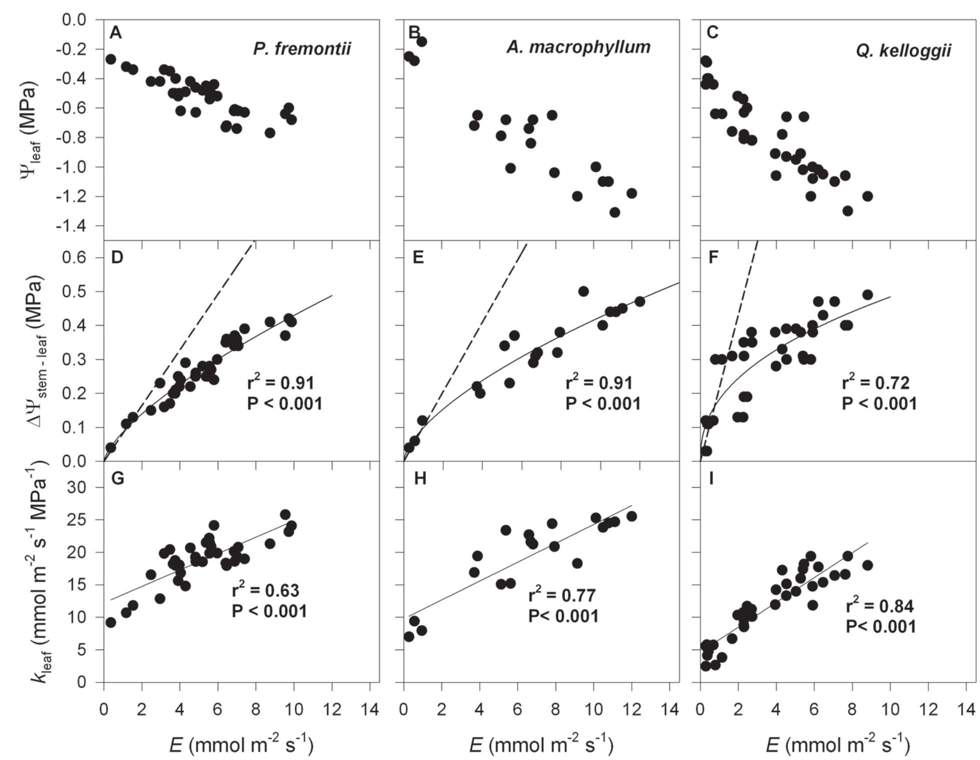

Fig. 3. Variation in leaf water potential (Ψ_{leaf}, MPa), the difference between stem and leaf water potential ($\Delta\Psi_{stem–leaf}$, MPa), and leaf hydraulic conductance (k_{leaf}, mmol m^{-2} s^{-1} MPa^{-1}) as a function of transpiration rate (E, mmol m^{-2} s^{-1}) for the three angiosperm species from the common garden: *P. fremontii* (A, D, G); *A. macrophyllum* (B, E, H); and *Q. kelloggii* (C, F, I). Solid and dashed lines, as well as r^2 and P values are as for Fig. 2.

Table 1. *Daytime maximum stomatal conducatance (g_s) and transpiration (E)±1 standard deviation for study species from the common garden*

The r^2 for the linear model describing the co-variation between k_{leaf} and E including the y-intercept ($k_{leaf(0)}$) and gain (dk_{leaf}/dE); for every species (P<0.001, for all species).

	Species	$g_{s,max}$ (mol m^{-2} s^{-1})	E_{max} (mmol m^{-2} s^{-1})	$k_{leaf(0)}$ (mmol m^{-2} s^{-1} MPa^{-1})	$k_{leaf(E)}$ (mmol m^{-2} s^{-1} MPa^{-1})	dk_{leaf}/dE (MPa^{-1})	k_{leaf} vs E
Angiosperms	*Acer macrophyllum*	0.47±0.13	11.2±1.55	9.77±1.43	25±0.48	1.45±0.19	r^2=0.77
	Populus fremontii	0.54±0.07	9.38±2.75	12.23±0.93	25.39±4.85	1.26±0.16	r^2=0.63
	Quercus kelloggii	0.27±0.07	5.18±1.15	4.66±0.65	17.83±1.41	1.91±0.14	r^2=0.84
Gymnosperms	*Metasequoia glyptostroboides*	0.12±0.05	1.93±0.42	2.95±0.44	8.01±1.20	2.26±0.35	r^2=0.62
	Pinus ponderosa	0.19±0.05	2.79±0.44	4.73±1.28	14.61±3.38	2.53±0.58	r^2=0.57
	Sequoia sempervirens	0.15±0.03	1.53±0.47	1.63±0.55	9.38±1.79	4.15±0.48	r^2=0.74

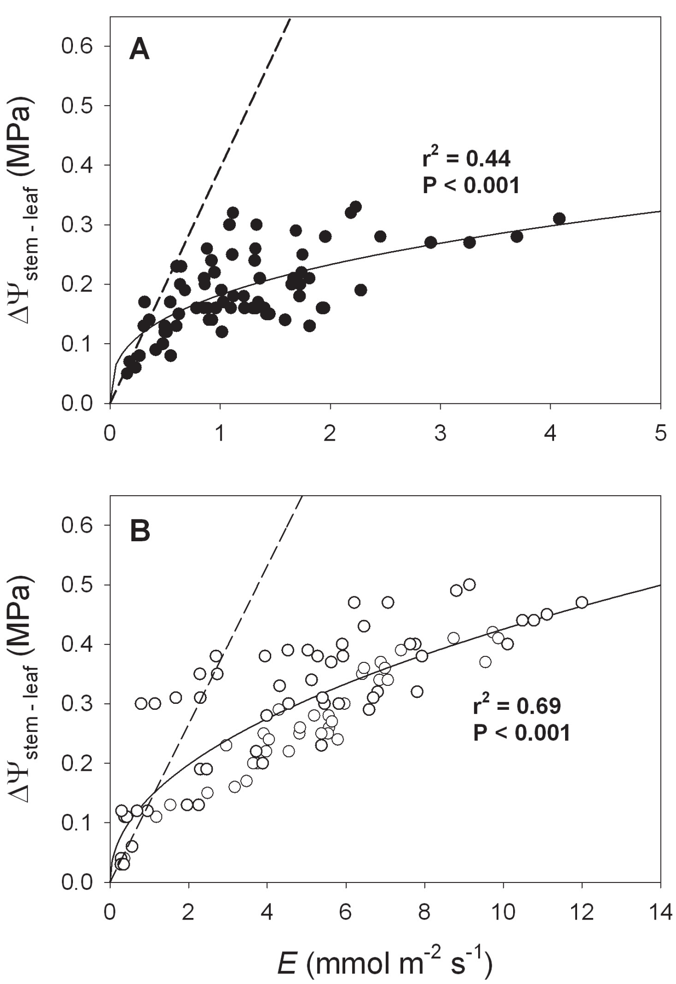

Fig. 4. The difference between stem and leaf water potential ($\Delta\Psi_{stem-leaf}$, MPa) as a function of transpiration rate (E, mmol m^{-2} s^{-1}) for: (A) gymnosperm and (B) angiosperm tree species from the common garden. Solid lines, as well as r^2 and P values are as for Fig. 2. The dashed lines represent the predicted changes in $\Delta\Psi_{stem-leaf}$ for a leaf that possesses the average static leaf hydraulic conductance (i.e. $k_{leaf(0)}$) for the (A) gymnosperm and (B) angiosperm species.

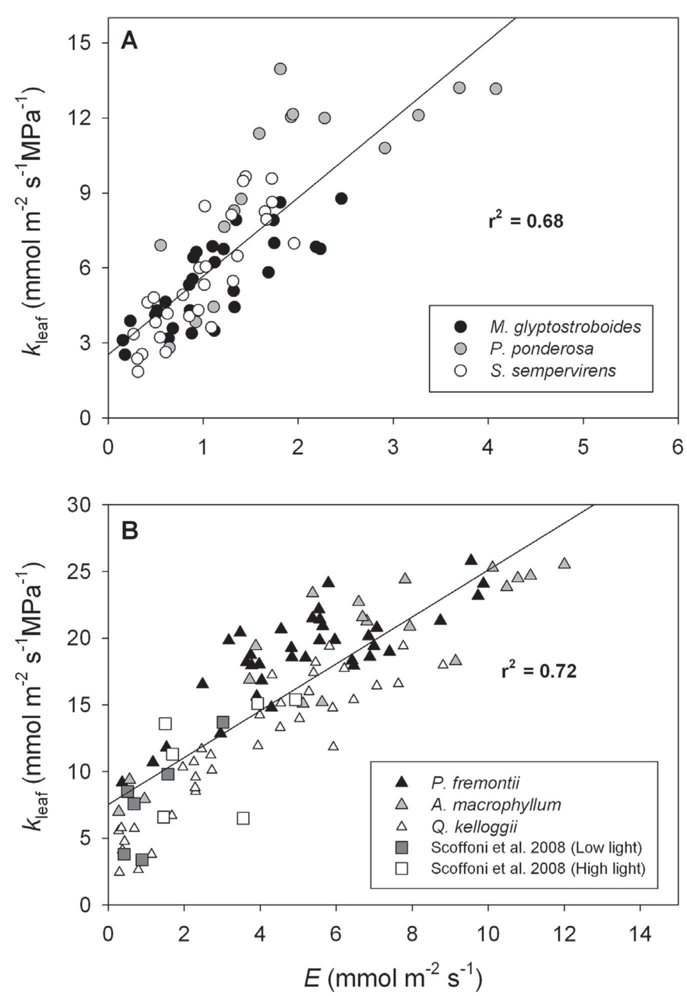

Fig. 5. Leaf hydraulic conductance (k_{leaf}, mmol m^{-2} s^{-1} MPa^{-1}) as a function of transpiration rate (E, mmol m^{-2} s^{-1}) for: (A) gymnosperm and (B) angiosperm tree species from the common garden. Previously published data taken from Table 2 in Scoffoni *et al.* (2008) is also shown as filled and open squares in B. Filled squares represent the k_{leaf} values taken when leaves were exposed to low light (<10 µmol m^{-2} s^{-1}), whereas the open squares represent the k_{leaf} values when leaves were exposed to high light (>1000 µmol m^{-2} s^{-1}; See Scoffoni *et al.* (2008) for further details). The solid line in each panel was fitted by linear regression through all the data, excluding the data by Scoffoni *et al.* (2008).

Table 1). The angiosperm species from the common garden operated at a higher day time maximum g_s and $\Delta\Psi_{stem-leaf}$ than the gymnosperm species (Figs 4, 6; Table 1).

Qualitatively similar diurnal trends in g_s, E, Ψ_{leaf}, Ψ_{stem}, and k_{leaf} were observed for the angiosperm and gymnosperm species grown in the common garden. In general, from dawn to midday, Ψ_{leaf} and Ψ_{stem} decreased while g_s, E, and k_{leaf} increased (Supplementary Figs S1 and S2). After midday, Ψ_{leaf} and Ψ_{stem} increased slightly,

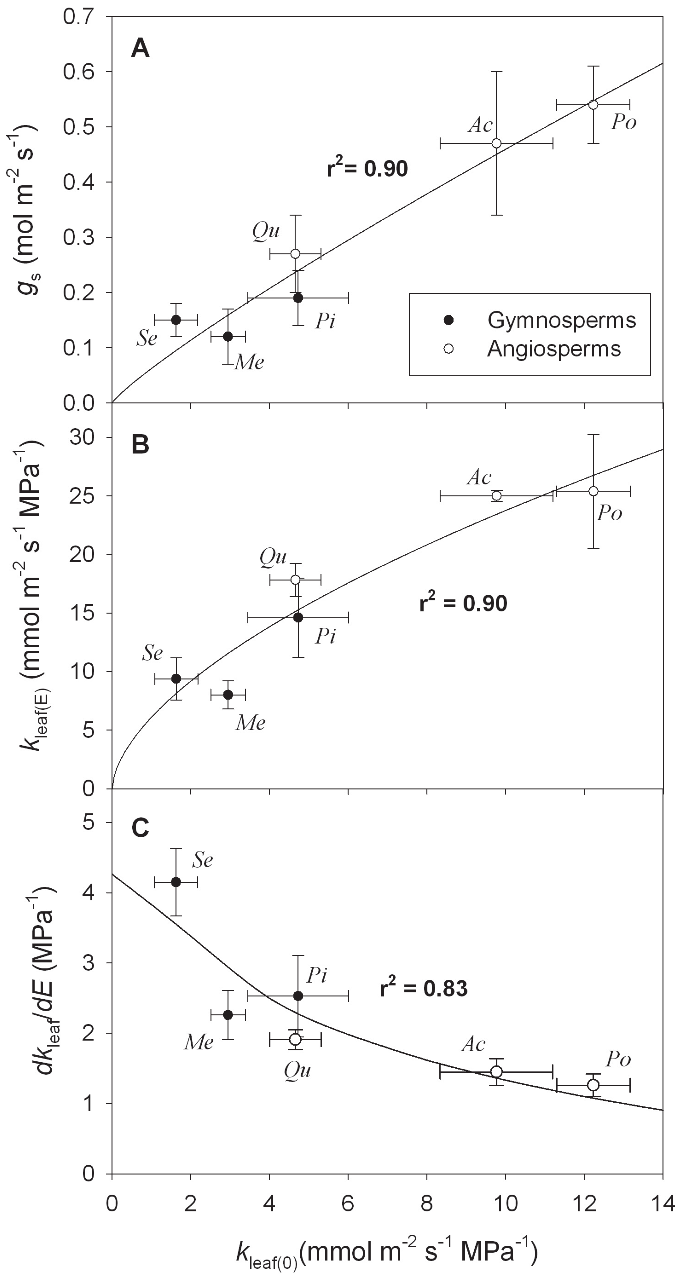

Fig. 6. The influence of static leaf hydraulic conductance ($k_{leaf(0)}$, mmol m^{-2} s^{-1} MPa^{-1}) on (A) maximum daytime stomatal conductance (g_s, mol m^{-2} s^{-1}); (B) maximum daytime leaf hydraulic conductance ($k_{leaf(E)}$, mmol m^{-2} s^{-1} MPa^{-1}), and (C) the slope of the linear relationship between $k_{leaf(E)}$ and E (i.e. the hydraulic gain) for three gymnosperm and three angiosperm species. *Se*, *Me*, *Pi*, *Qu*, *Ac* and *Po* are *Sequoia sempervirens*, *Metasequoia glyptostroboides*, *Pinus ponderosa*, *Quercus kelloggii*, *Acer macrophyllum*, and *Populus fremontii*, respectively. Solid lines represent the best-fit model describing the coordination between g_s, $k_{leaf(E)}$ and dk_{leaf}/dE with variation in $k_{leaf\ (0)}$.

whereas g_s, E, and k_{leaf} decreased (Supplementary Figs S1 and S2). Overall, plants in the common garden were well hydrated, with Ψ_{stem} and Ψ_{leaf} greater than –0.8 and –1.2 MPa, respectively. The diurnal changes in Ψ_{leaf} and Ψ_{stem} followed a similar pattern such that $\Delta\Psi_{stem\text{-}leaf}$ changed very little over the course of a day (Supplementary Figs S1 and S2). On average the angiosperm species showed greater diurnal variation in g_s, E, and k_{leaf} compared with the gymnosperm species (Supplementary Figs S1 and S2).

Growth chamber

Across all three CO_2 treatments a similar range of E, VPD, A, T_{leaf}, and g_s, occurred at each light level (Fig. 7A–E). Overall, PAR had the greatest significant effect on g_s (F=31.85, P<0.001) followed by VPD (F=8.55, P=0.012) and CO_2 (F=7.7281, P=0.0129) with no significant interaction between PAR, CO_2, and VPD. Across CO_2 treatments, increases in PAR were associated with greater g_s (t=5.64, P<0.001; Fig. 7E). On average, plants grown under sub-ambient CO_2 operated at higher g_s than plants from elevated CO_2 (t=3.95, P=0.002) but were not statistically different from plants grown under ambient CO_2 (t=1.89, P=0.08). Although VPD showed a significant main effect on g_s, correlations between g_s and VPD within each CO_2 treatment were not significantly different, which was probably due to the small range of VPD and limited number of measurements at different VPD (n=5) at a given light level. Both PAR (F=31.49, P<0.001) and CO_2 (F=9.76, P<0.002) significantly influenced variation in A. Across treatments, increasing PAR had a positive effect on A (t=5.612, P<0.001). Similar to g_s, when measured at the same atmospheric CO_2 concentration (450 ppm), plants from the sub-ambient CO_2 treatment showed higher A than plants from the elevated CO_2 treatment (t=4.24, P=0.001) but were not statistically different from the ambient CO_2 treatment (t=0.89, P=0.39). Using an ANCOVA to test for main and interactive effects of CO_2, light, and E on k_{leaf}, it was found that E had the only significant effect on k_{leaf} (F=16.1945, P=0.0027).

Across all CO_2 treatments an increase in E was associated with a decrease in Ψ_{leaf}, although the decreases in Ψ_{leaf} were relatively minor despite relatively large variation in E (Fig. 8A). Similar to plants from the common garden, a strong non-linear relationship between $\Delta\Psi_{stem\text{–}leaf}$ and E was observed across all three growth CO_2 treatments ($y=0.106\times E^{0.507}$, r^2=0.77, P<0.001; Fig. 8B; assuming that the when E=0, $\Delta\Psi_{stem\text{–}leaf}$=0). This was the result of a significant positive relationship between k_{leaf} and E across all three CO_2 treatments ($y=9.70 + 2.36\times E$, r^2=0.72; Fig. 9B). The lack of interactive effects between E and CO_2 on k_{leaf} suggests that $k_{leaf(0)}$ was not significantly influenced by growth CO_2 (Table 2). Similarly, k_{leaf} per unit g_s and A were relatively unaffected by PAR, but were significantly, positively correlated with VPD (k_{leaf}/g vs. VPD: $y=0.0281\times e^{(0.5355\times \mathrm{VPD})}$, r^2=0.23, P=0.009; k_{leaf}/A vs. VPD: $y=0.4837\times e^{(0.4634\times \mathrm{VPD})}$, r^2=0.30, P=0.002).

Discussion

The data presented here do not support a constant k_{leaf} model, under well-watered conditions, and instead are consistent with a hydraulic mechanism whereby k_{leaf} increases with E. Additionally, here it is shown that a positive dependence of k_{leaf} on E results in a dynamic coupling between k_{leaf} and g_s that ultimately minimizes the water potential drawdown across the leaf (i.e. $\Delta\Psi_{stem\text{–}leaf}$) which, via the hydraulic feedback loop, increases the maximum potential g_s and A for a given VPD (Fig. 10).

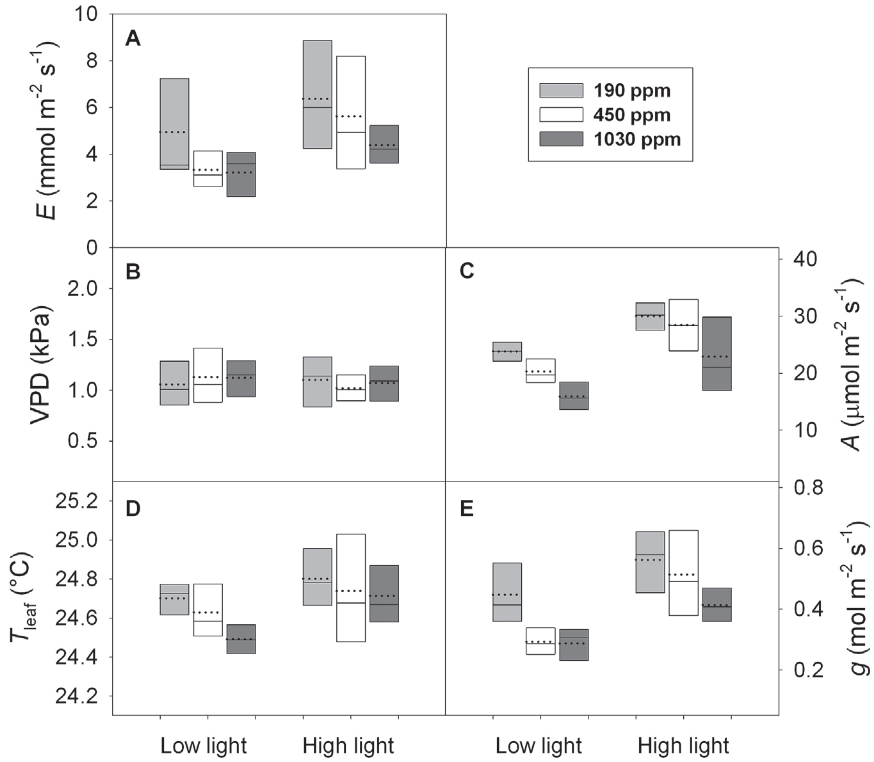

Fig. 7. The range (indicted by boxes), median (horizontal line within boxes), and mean (dotted line within boxes) of: (A) transpiration rate (E, mmol m^{-2} s^{-1}), (B) leaf-to-air vapour pressure difference (VPD, kPa), (C) CO_2 assimilation rate (A, μmol m^{-2} s^{-1}), (D) leaf temperature (T_{leaf}, °C), and (E) leaf surface conductance, comprising the sum of stomatal and boundary layer conductances g_s and g_b (g, mol m^{-2} s^{-1}) during measurements of leaf hydraulic conductance (k_{leaf}) at both low (500 μmol m^{-2} s^{-1} PAR) and high light (1300 μmol m^{-2} s^{-1} PAR), for *H. annus* plants grown under ~190 (grey boxplot), 450 (open boxplot), and 1030 ppm CO_2 (dark grey boxplot). Note that here, g_b is considered sufficiently high such that $g \approx g_s$.

Static vs dynamic leaf hydraulic conductance

At steady-state, the coupling between liquid and vapour-phase water flux can be described as:

$$k_{leaf}(\Delta\Psi_{stem\text{-}leaf}) = g(w_i - w_a) = g(e_i - e_a)/P \qquad (2)$$

where g is the sum of stomatal (g_s) and boundary layer conductance (g_b) to water vapour in series, w_i and w_a are the mole fractions of water vapour (mol mol^{-1}) inside the leaf and of the ambient atmosphere, e_i and e_a are the vapour pressures of water inside the leaf and in ambient air, and P is atmospheric pressure. The term $(e_i–e_a)/P$ is commonly referred to as 'VPD'. According to this steady-state description, when $g_s << g_b$, up- or down-regulation of E via feedback responses of stomata to VPD can occur via changes in $\Delta\Psi_{stem–leaf}$, k_{leaf}, or both.

If k_{leaf} is static or only decreases as E increases then changes in g_s and E, before water-stressed-induced xylem embolism, would require large changes in $\Delta\Psi_{stem–leaf}$ and ultimately a positive linear correlation between $\Delta\Psi_{stem–leaf}$ and $g(w_i - w_a)$ or E (Fig. 1). From Eqn 2, when k_{leaf} is static, the ratio $g(w_i–w_a)/\Delta\Psi_{leaf}$ remains constant. Eventually, increases in $g(w_i–w_a)$ may lower leaf water potential sufficiently to induce cavitation and embolisms, reducing k_{leaf} and resulting in a positive feedback on $\Delta\Psi_{stem–leaf}$ (Sperry, 2000). In this scenario $g(w_i–w_a)/\Delta\Psi_{leaf}$ is negatively correlated with E. Because increasing $\Delta\Psi_{stem–leaf}$ reduces maximum potential g and by extension CO_2 assimilation rate (Buckley, 2005; Franks *et al.*, 2007), a control system that relies solely on a constant or decreasing k_{leaf} constrains carbon gain to occur within a relatively narrow range of low evaporative demand and high water availability. One way to avoid large drops in Ψ_{leaf} and g over a broad range of evaporative demand is to vary k_{leaf} positively with E. This dynamic coupling between E and k_{leaf} is represented here by the term $k_{leaf(E)}$, which is the leaf hydraulic conductance for a given magnitude of E. Here, $k_{leaf(E)}$ represents the dynamic hydraulic conductance.

Under relatively well-watered conditions no support was found for the hypothesis that $g(w_i–w_a)/\Delta\Psi_{leaf}$ is constant or decreases with E. In fact the opposite relationship was observed: as E increased $g(w_i–w_a)/\Delta\Psi_{leaf}$ increased (e.g. Figs 2, 3 and 8). As shown by Eqn 2, a positive dependence of k_{leaf} on E can lead to increasing $g(w_i–w_a)/\Delta\Psi_{leaf}$ as E increases. Therefore, these results provide strong evidence that the relationship between k_{leaf}, g_s, and CO_2 assimilation rate, in response to short-term changes in evaporative demand (VPD), is the result of a positive dependence of k_{leaf} on E (Fig. 10).

Co-variation between $\Delta\Psi_{stem–leaf}$, E, g_s, and k_{leaf} over a diurnal cycle of evaporative demand

Previous research has provided evidence that diurnal variation in k_{leaf} can be partially attributed to circadian regulation (Nardini *et al.*, 2005*b*; Lo Gullo *et al.*, 2005). Here evidence is provided that a positive correlation between k_{leaf} and E is

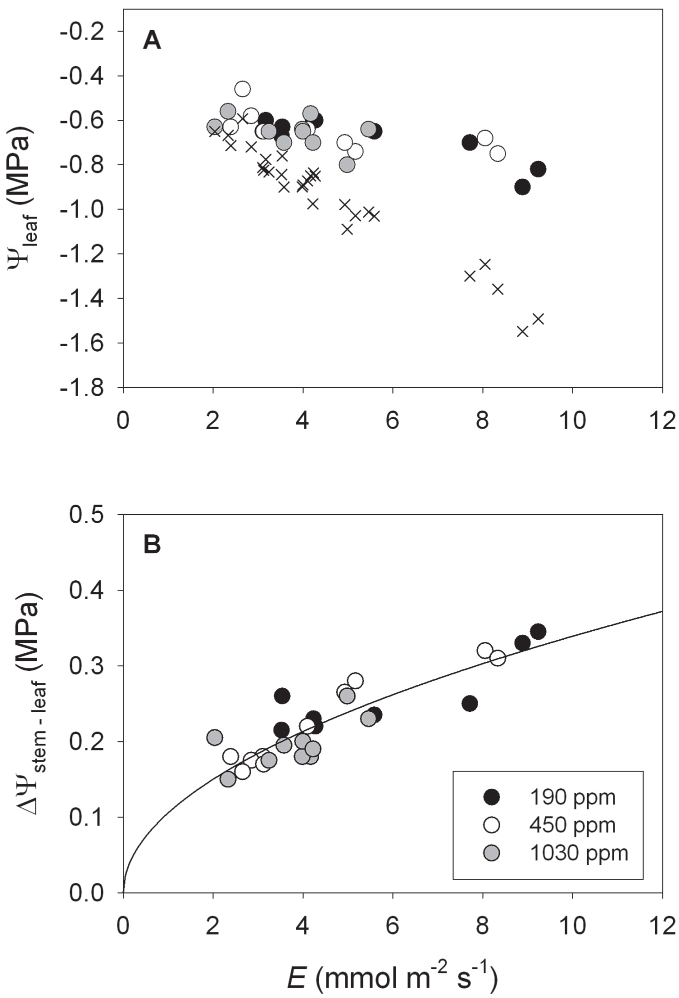

Fig. 8. The influence of variation in transpiration rate (E, mmol m^{-2} s^{-1}) on (A) leaf water potential and (B) the difference between stem and leaf water potential ($\Delta\Psi_{stem–leaf}$, MPa) for: *H. annus* plants grown under ~190 (filled circles), 450 (open circles), and 1030 ppm CO_2 (grey circles). The crosses in A represent the predicted leaf water potentials for a leaf that possesses the average static leaf hydraulic conductance (i.e. $k_{leaf(0)}$=9.08 mmol m^{-2} s^{-1} MPa^{-1}) across all three CO_2 treatments. The solid black line in panel (B) represents the best-fit model describing the coordination between $\Delta\Psi_{stem–leaf}$ and E.

another factor influencing the coupling between k_{leaf} and g_s over a diurnal cycle of evaporative demand. Despite relatively large diurnal variation in g_s and E for the gymnosperm and angiosperm species growing in a common garden, only minor variation was observed in $\Delta\Psi_{stem–leaf}$ across a large range in E. Until now, isohydrodynamic behaviour, or a relatively constant water potential gradient, has only been explained by a mechanism occurring at the whole plant level, from root to leaf, over seasonal changes in soil water availability (Franks *et al.*, 2007). The data presented here suggest that, under well-watered conditions, isohydrodynamic behaviour is common at the leaf level (e.g. Figs 2, 3, 8b). As described by Eqn 1 and 2, a minor variation in $\Delta\Psi_{stem–leaf}$ over a large diurnal range in E and g_s, can occur if k_{leaf} is positively dependent on E.

Similar to an electrical circuit that maintains an electrical conductance even when there is no current, if a hydraulic connection exists between plants and the atmosphere then leaves will maintain the capacity to transport water, even when E=0. In other words, whether k_{leaf} is dynamically coupled to E ($k_{leaf(E)}$) or static, it has a finite value when E=0, i.e. $k_{leaf(0)}$ (see Methods). Here it is shown that, for the well-watered gymnosperm and angiosperm tree species in the common garden, this inherent capacity to transport water is greater for the angiosperm species than the gymnosperms (Fig. 6), and positively correlated with daytime maximum stomatal conductance (Fig. 6A). These patterns are consistent with the well-documented 'coordination' of hydraulic and gas exchange capacity across species (e.g. Meinzer and Grantz, 1990; Meinzer and Grantz, 1991; Sperry and Pockman, 1993; Winkel and Rambal, 1993; Meinzer *et al.*, 1995; Andrade *et al.*, 1998; Maherali *et al.*, 1997; Mencuccini and Comstock, 1999; Mencuccini, 2003; Brodribb *et al.*, 2005).

Influence of atmospheric CO_2 on the co-variation between $\Delta\Psi_{stem–leaf}$, E, g_s, A, and k_{leaf}

Across all three growth CO_2 treatments a strong non-linear relationship was observed between $\Delta\Psi_{stem–leaf}$ and E where $g(w_i–w_a)/\Delta\Psi_{leaf}$ increased as E increased. As with plants from

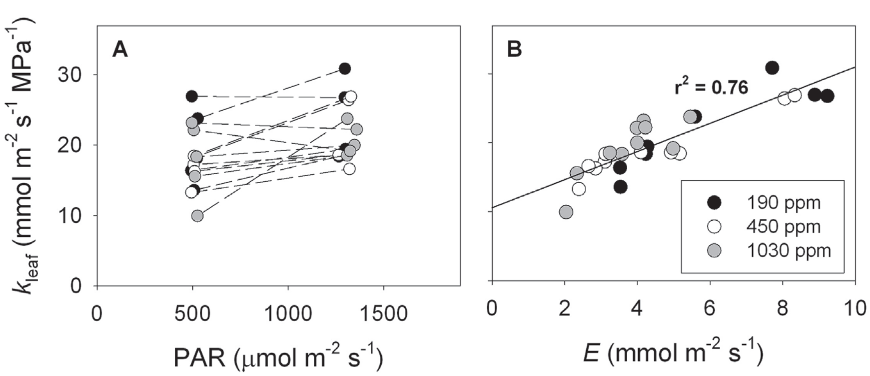

Fig. 9. The influence of variation in: (A) photosynthetically active radiation (PAR, µmol m^{-2} s^{-1}) and (B) transpiration rate (E, mmol m^{-2} s^{-1}) on leaf hydraulic conductance (k_{leaf}, mmol m^{-2} s^{-1} MPa^{-1}). The dotted lines in A show the 'light–g-effect' on k_{leaf} for leaves at a common leaf to air vapour pressure difference (VPD). In all cases where greater light interception resulted in an increase in k_{leaf}, at a common VPD, there was a light induced increase in g and by extension E.

Table 2. *Mean stomatal conducatance (g_s) and transpiration (E)±1 standard deviation for* H. annus *plants grown under ~190, 450, and 1030 ppm CO_2. Also shown are the hydraulic gain (dk_{leaf}/dE) and the y-intercept ($k_{leaf}(0)$) and r^2 for the linear model describing the co-variation between k_{leaf} and E (k_{leaf} vs E)*

*$P < 0.001$; **$P < 0.01$.

Growth CO_2 (ppm)	Mean g_s (mol m^{-2} s^{-1})	*Mean E* (mmol m^{-2} s^{-1})	$k_{leaf(0)}$ (mmol m^{-2} s^{-1} MPa^{-1})	dk_{leaf}/dE (MPa^{-1})	k_{leaf} vs *E*
190±35	0.50±0.12	5.57±2.41	9.75±2.44	2.12±0.41	r^2=0.80*
450±46	0.40±0.15	0.54±0.07	9.38±2.75	12.23±0.93	r^2=0.91*
1030±74	0.35±0.09	0.27±0.07	5.18±1.15	4.66±0.65	r^2=0.70**

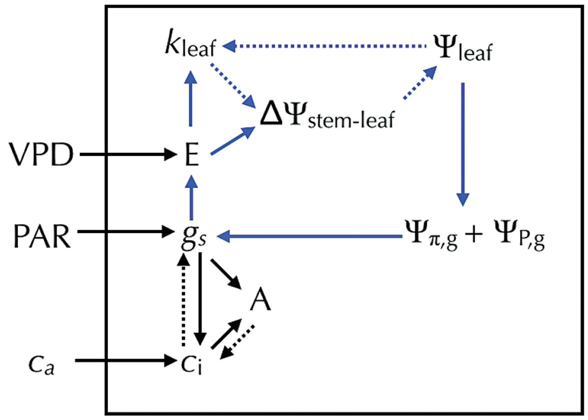

Fig. 10. Model diagram showing the coordination between transpiration rate (*E*), the difference between stem and leaf water potential ($\Delta\Psi_{stem-leaf}$), leaf hydraulic conductance (k_{leaf}), stomatal conductance (g_s, where boundary layer conductance g_b is sufficiently high for g_s to dominate), and CO_2 assimilation rate (*A*). The blue lines represent the hydraulic feedback loop between g_s and *E*. Solid lines represent a positive relationship between parameters and dotted lines represent a negative relationship. The positive relationship between *E* and k_{leaf} is the predicted relationship based on data gathered from *H. annuus* plants grown under low, medium, and high CO_2 concentrations, and three gymnosperm and angiosperm tree species growing in a common garden (see Methods for more detail). The black box indicates the boundary between leaf processes and external environmental variables. (VPD, leaf-to-air vapour pressure difference; PAR, photosynthetically active radiation; C_a, atmospheric CO_2 concentration, C_i, leaf internal CO_2 concentration, $\Psi_{\pi,g}$, is the guard cell osmotic pressure, and $\Psi_{P,g}$, guard cell turgor pressure).

the common garden experiment, this trend can be attributed to a positive correlation between k_{leaf} and *E* which was relatively decoupled from variation in PAR (Fig. 9). Recent research relying on the evaporative flux method provides further evidence that k_{leaf} can be up-regulated as transpiration increases (e.g. Scoffoni *et al.*, 2008; Guyot *et al.*, 2011). In this previous work, unlike the present evaluation, increases in transpiration rate were driven by a g_s light response. As reported here, a positive dependence of k_{leaf} on *E* can occur independent of variation in light availability. This suggests that an alternative mechanism is necessary to describe the coordination between k_{leaf} and light. For example, an isohydroynamic model predicts greater k_{leaf} as light interception increases if increased energy absorption results in greater *E* (see Figs 9 and 10).

The positive linear model describing the relationship between k_{leaf} and *E* was similar across the CO_2 treatments such that $k_{leaf(0)}$ was relatively conserved between CO_2 treatments (Fig. 9B, Table 2). However, variation in growth CO_2 influenced where plants operated along the linear model describing the co-variation between k_{leaf} and *E*, with a lower maximum k_{leaf} and *E* at high ambient CO_2. Corresponding with this, average g_s was lower in the elevated CO_2 treatment relative to the sub-ambient CO_2 treatment, consistent with many studies on plants growing under different atmospheric CO_2 concentrations (e.g. Morison and Gifford, 1983; Cure and Acock, 1986; Tolley and Strain, 1985; Morison and Lawlor, 1999).

The relative stability of $k_{leaf(0)}$ across sub-ambient, ambient, and elevated CO_2 treatments despite a significant decrease in g_s between sub-ambient and elevated CO_2 is consistent with previous research. Across species, the sensitivity of maximum stomatal conductance ($g_{s(max)}$) to variation in atmospheric CO_2 (c_a) seems to be strongly non-linear whereby the sensitivity of $g_{s(max)}$ to changes in c_a increases at low c_a (Beerling and Woodward, 1997; Franks and Beerling, 2009; Franks *et al.*, 2012). Recent research also suggests that the relative differences in g_s between plants grown under sub-ambient, ambient, and elevated CO_2 is less for plant species that possess an inherently high g_s (Franks *et al.*, 2012). Additionally, across species, there is a strong non-linear relationship between g_s and k_{leaf}, when measured at a common VPD, whereby dg_s/dk_{leaf} increases as g_s increases (Franks, 2006). Taken together, this previous research suggests that plants with an inherently high g_s and k_{leaf} will show relatively minor adjustments in $g_{s(max)}$ and $k_{leaf(0)}$ when exposed to elevated CO_2, as shown here with the *H. annuus* plants. Similarly, recent research on soybean suggests that k_{leaf} is relatively insensitive to elevated CO_2 (700 ppm) despite decreases in g_s at elevated CO_2 (Locke *et al.*, 2013). Further research, including more species and greater ranges of CO_2, is necessary to better understand the influence of elevated atmospheric CO_2 on the coordination between *E*, k_{leaf}, g_s, and *A*.

The hydraulic gain, dk_{leaf}/dE, and the sensitivity of g_s to E

Previous research has clearly demonstrated a hydromechanical basis for stomatal movement whereby changes in the maximum potential aperture of stomata and by extension g_s are strongly influenced by changes in bulk leaf water status i.e. Ψ_{leaf} (see reviews by Franks, 2004; Buckley, 2005). This hydraulic coupling between maximum potential g_s and Ψ_{leaf} results in a hydromechanical control system that is strongly influenced by both *E* and k_{leaf}. For example, a hydromechanical stomatal control system that includes a positive dependence of k_{leaf} on E will reduce the sensitivity of Ψ_{leaf} to variation in E, when compared with a constant k_{leaf} (e.g. Fig. 8A) This can be shown mathematically by:

$$\Psi_{leaf} = \Psi_{stem} - \left(\frac{E}{k_{leaf(0)} + \left(\frac{dk_{leaf}}{dE} \times E \right)} \right) \text{ for a dynamic } k_{leaf}$$

model compared with $\Psi_{leaf} = \Psi_{stem} - \left(\frac{E}{k_{leaf(0)}} \right)$ for a static k_{leaf} model. This damping of variation in Ψ_{leaf} as E changes is expected to reduce the sensitivity of g_s to changes in VPD via the hydraulic feedback loop (Fig. 10). In other words, the rate and direction of change in the ratio of k_{leaf} on E (here this is termed the hydraulic gain; dk_{leaf}/dE) is a good index of the sensitivity of leaf water status (i.e. Ψ_{leaf}) and g_s to a change in E.

Using a hydromechanical model of g_s, originally developed by Franks and Farquhar (1999) and further modified by Franks *et al.* (2007) to accommodate isohydrodynamic behaviour (i.e. decrease in $\Delta\Psi_{stem-leaf}/E$, as E increases), the impact of a dynamic conductance ($k_{leaf(E)}$), as compared with a static k_{leaf}, on the sensitivity of g_s to changes in VPD was evaluated. The model output suggests that, for well-hydrated plants with a fixed Ψ_{stem}, a positive dependence of k_{leaf} on E reduces the sensitivity of g_s to variation in VPD when compared with a constant k_{leaf} (Fig. 11). Previous research has provided strong empirical evidence that stomatal sensitivity to VPD is positively correlated with the daytime operating g_s under well watered conditions at low VPD, i.e.<1kPa (e.g. Oren *et al.*, 1999). Similarly, across species from the common garden a strong negative correlation was observed between dk_{leaf}/dE and $k_{leaf(0)}$, with $k_{leaf(0)}$ positively correlated with daytime maximum g_s (Fig. 6A, C). Taken together, the steady-state stomatal feedback control model proposed by Franks *et al.* (2007) and the negative correlation between dk_{leaf}/dE and $k_{leaf(0)}$ observed here provide a mechanistic framework for evaluating empirical correlations between stomatal sensitivity to VPD and daytime operating g_s under well-watered conditions at low VPD. Further research is needed to better characterize the coordination between $k_{leaf(0)}$, dk_{leaf}/dE, maximum g_s, and stomatal sensitivity to VPD across plants spanning a wide range in maximum potential g_s.

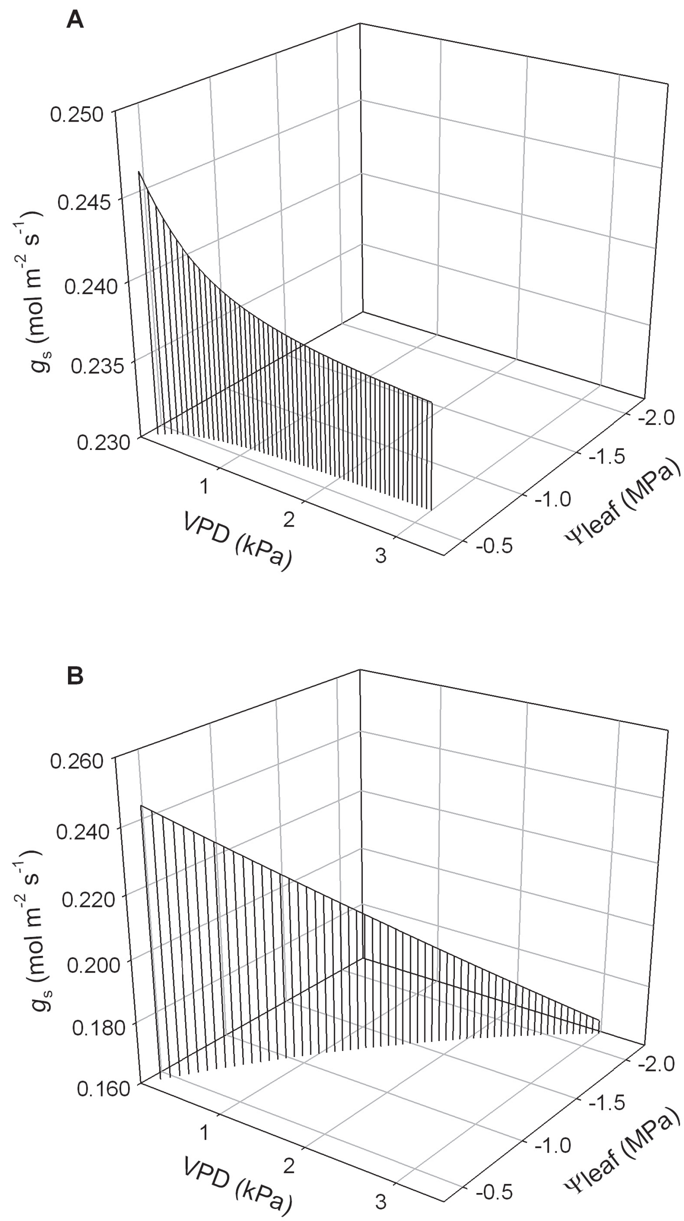

Fig. 11. Model simulations comparing the relationship between leaf water potential (Ψ_{leaf}), leaf to air vapour pressure difference (VPD), and stomatal conductance (g_s) when: (A) leaf hydraulic conductance (k_{leaf}) is positively dependent on transpiration rate (E), based on the empirical relationship observed across the gymnosperm species in the common garden experiment (see Fig. 5) where k_{leaf}=2.5+3.2×E, and (B) a constant k_{leaf} based on the y-intercept of the combined gymnosperm data (i.e. $k_{leaf(0)}$=2.5). Note that in A, Ψ_{leaf} remains high as VPD increases, whereas in (B) Ψ_{leaf} declines substantially with increasing VPD.

Possible processes underlying the variable k$_{leaf}$ mechanism

It is now well recognized that k_{leaf} and leaf gas exchange are strongly influenced by variation in leaf vein traits (e.g. Brodribb *et al.*, 2007; Blonder *et al.*, 2011; Sack and Scoffoni, 2013). Although changes in xylem structure will directly impact the inherent hydraulic capacity of a leaf (e.g. $k_{leaf(0)}$) it is unlikely that short-term increases in E and $k_{leaf,}$ when leaves are well-hydrated, are driven by up-regulation of xylem hydraulic conductance alone. Changes in the ion concentrations of stem xylem sap have been shown to significantly influence stem hydraulic conductance (e.g. Zwieniecki *et al.*, 2001; Nardini *et al.*, 2011). Yet, to date, this ion effect has not been found in leaves (Sack *et al.*, 2004). Instead, leaf xylem hydraulic conductance, prior to any form of xylem dysfunction, is relatively constant and independent of short-term variation in evaporative demand, excluding any temperature effects on viscosity.

In contrast to that of the leaf xylem, there is growing evidence that the hydraulic conductance of the extra-xylem pathway can ramp up or down over relatively short time scales in response to changes in a particular environmental cue, such as light, temperature or water availability (e.g. Kikuta *et al.*, 1997; Sôber, 1997; Matzner and Comstock, 2001; Lo Gullo *et al.*, 2005; Sellin and Kupper, 2005*a*,*b*; Cochard *et al.*, 2007; Sellin and Kupper, 2007; Scoffoni *et al.*, 2008; Sellin *et al.*, 2008; Johnson *et al.*, 2009; Pantin *et al.*, 2012). However, as changes in light and temperature can have direct effects on *E*, the data presented here suggests that a similar range of *E* should be maintained when testing for light and temperature effects on the hydraulic conductance of the extra-xylem pathway independent of variation in *E*. To date, the relative contribution of symplastic, transcellular, and apoplastic water transport through the extra-xylary tissues is still under debate (e.g. Tyree and Cheung, 1977; Tyree *et al.*, 1981; Johansson *et al.*, 1996; Morillon and Chrispeels, 2001; Aasamaa *et al.*, 2005; Aroca *et al.*, 2006; Cochard *et al.*, 2004; Cochard *et al.*, 2007; Kim and Steudle, 2007; Sellin *et al.*, 2008; Baaziz *et al.*, 2012; Rockwell *et al.*, 2014), as is the extent to which the different live tissues of a leaf (e.g. palisade and spongy mesophyll, bundle sheath, epidermis) participate in the transpiration stream (e.g. Zwieniecki *et al.*, 2007; Canny *et al.*, 2012).

Clearly one of the missing pieces of the puzzle is the location of the site(s) of evaporation inside the leaf (Pieruschka *et al.*, 2010; Peak and Mott, 2011). It is difficult to evaluate water transport through the extra-xylary pathways in the leaf if there is no clear understanding of where the liquid flow path ends and whether or not the locations of these evaporation sites vary with changes in the absolute rate of leaf water loss (i.e. *E*). For example, recent research suggests that vapour transport through the intercellular air spaces can account for a substantial amount of water transport between mesophyll cells and thus the hydraulic conductance of the extra-xylary component (Rockwell *et al.*, 2014; Buckley, 2014). Additionally, changes in *E* may shift the depth of the evaporation front within leaves (Rockwell *et al.*, 2014; Buckley, 2014) and alter the relative contribution of liquid and vapour transport through these parallel pathways within the mesophyll. Characterizing where the evaporation sites occur in the leaf is needed to fully understand how water transport through the mesophyll is partitioned between these parallels pathways (i.e. liquid–apoplastic, symplastic, transcellular; vapour–intercellular air spaces).

Conclusions

The results presented here suggest that when plants are well-hydrated, k_{leaf} does not remain fixed or decrease as *E* increases, but rather increases with *E*. Here, this dynamic k_{leaf} is referred to as $k_{leaf(E)}$, which incorporates the inherent k_{leaf} at zero *E*, $k_{leaf(0)}$. This positive dependence of k_{leaf} on *E* tends to minimize or reduce water potential gradients along the soil–plant–atmosphere continuum. Minimizing variation in $\Delta\Psi_{stem-leaf}$ over a broad range of *E* (i.e. maintaining isohydrodynamic conditions), and therefore maximizing leaf water content (LWC), has many potential implications for whole plant carbon balance. It is well recognized that decreases in Ψ_{leaf} and LWC can increase stomatal and biochemical limitations to CO_2 assimilation rate (*A*) and thus decrease potential *A* for given environmental conditions (Lawlor, 2002; Lawlor and Cornic, 2002). A positive dependence of k_{leaf} on *E* will ultimately increase the range of stem water potentials where leaves can maintain water potential above the turgor loss point, supporting high LWC, g_s, and *A*. This mechanism will dominate only while the xylem remains hydraulically intact, i.e. in well-hydrated leaves. As Ψ_{leaf} falls below the cavitation threshold the subsequent drop in k_{xylem} will dominate and the leaf will exhibit the classical pattern of falling *E* with declining k_{leaf}. Minimizing $\Delta\Psi_{stem-leaf}$ avoids other negative consequences of excessive water potential gradients such as reduced rates of export of photoassimilates from leaves (Nikinmaa *et al.*, 2013; Turgeon, 2010; Hölttä *et al.*, 2009; Hölttä *et al.* 2006; Thompson and Holbrook, 2004). The dynamic nature of k_{leaf} is therefore integral to many aspects of plant water use and productivity and should be considered in mechanistic vegetation models.

Supplementary data

Supplementary data are available at *JXB* online.

Figure S1. Diurnal variation in photosynthetically active radiation (PAR, μmol m^{-2} s^{-1}), stomatal conductance (*g*s, mol m^{-2} s^{-1}), stem and leaf water potential (Ψstem and Ψleaf, MPa), leaf hydraulic conductance (*k*leaf, mmol m^{-2} s^{-1}) and transpiration rate (*E*, mmol m^{-2} s^{-1}) for three angiosperm species growing in a common garden.

Figure S2. Diurnal variation in photosynthetically active radiation (PAR, μmol m^{-2} s^{-1}), stomatal conducatance (*g*s, mol m^{-2} s^{-1}), stem and leaf water potential (Ψstem and Ψleaf, MPa), leaf hydraulic conductance (*k*leaf, mmol m^{-2} s^{-1}), and transpiration rate (*E*, mmol m^{-2} s^{-1}) for three gymnosperm species growing in a common garden.

Acknowledgements

We thank UC Berkeley Botanical Garden for providing the space necessary to conduct the field experiments. We thank Greg Goldsmith, Adam Roddy and Michal Shuldman for their help with measurements at the Berkeley Botanical Garden and Feike Dijkstra for comments that greatly improved the manuscript. We also thank the anonymous reviewers for the valuable feedback. Financial support was provided by a UC Berkeley BASC grant (UC Berkeley) awarded to KS.

References

Aasamaa K, Niinemets Ü, Sõber A. 2005. Leaf hydraulic conductance in relation to anatomical and functional traits during *Populous tremula* leaf ontogeny. *Tree Physiology* **25,** 1409–1418.

Andrade JL, Meinzer FC, Goldstein G, Holbrook NM, Cavelier J, Jackson P, Silvera K. 1998. Regulation of water flux through trunks, branches and leaves in tress of a lowland tropical forest. *Oecologia* **115,** 463–471.

Aroca R, Ferrante A, Vernieri P, Chrispeels MJ. 2006. Drought, abscisic acid, and transpiration rate effects on the regulation of PIP aquaporin gene expression and abundance in *Phaseolus vulgaris* plants. *Annals of Botany* **98,** 1301–1310.

Baaziz KB, Lopez D, Rabot A, Combes D, Gousset A, Bouzid S, Cochard H, Sakr S, Venisse J-S. 2012. Light mediated K_{leaf} induction and contribution of both the PIP1s and PIP2s aquaporins in five tree species: walnut (*Juglans regia*) case study. *Tree Physiology* **32,** 423–434.

Beerling DJ, Woodward FI. 1997. Changes in land plant function over the Phanerozoic: reconstructions based on the fossil record. *Botonical Journal of the Linnean Society* **124,** 137–153.

Black CR. 1979. The relationship between transpiration rate, water potential, and resistances to water movement in Sunflower (*Helianthus annuus* L.) *Journal of Experimental Botany* **30,** 235–243.

Blackman CJ, Brodribb TJ, Jordan GJ. 2009. Leaf hydraulics and drought stress: response, recovery and survivorship in four woody temperate plant species. *Plant, Cell and Environment* **32,** 1584–1595.

Blonder B, Violle C, Bentley LP, Enquist BJ. 2011. Venation networks and the origin of the leaf economics spectrum. *Ecology Letters* **14,** 91–100.

Brodribb TJ, Feild TS, Jordan GJ. 2007. Leaf maximum phosotynthetic rate and venation are linked by hydraulics. *Plant Physiology* **144,** 1890–1898.

Brodribb TJ, Holbrook NM. 2003. Changes in leaf hydraulic conductance during leaf shedding in seasonally dry tropical forest. *New Phytologist* **158,** 295–303.

Brodribb TJ, Holbrook NM. 2006. Declining hydraulic efficiency as transpiring leaves desiccate: two types of response. *Plant, Cell and Environment* **29,** 2205–2215.

Brodribb TJ, Holbrook NM, Zwieniecki MA, Palma B. 2005. Leaf hydraulic capacity in ferns, conifers and angiosperms: impacts on photosynthetic maxima. *New Phytologist* **165,** 839–846.

Buckley TN. 2005. The control of stomata by water balance. *New Phytologist* **168,** 275–292.

Buckley TN. 2014. The contributions of apoplastic, symplastic and gas phase pathways for water transport outside the bundle sheath in leaves. *Plant, Cell and Environment*. doi: 10.1111/pce.12372

Canny M, Wong SC, Huang C, Miller C. 2012. Differential shrinkage of mesophyll cells in transpiring cotton leaves: implications for static and dynamic pools of water, and for water transport pathways. *Functional Plant Biology* **39,** 91–102.

Cochard H, Coll L, Le Roux X, Améglio T. 2002. Unraveling the effects of plant hydraulics on stomatal closure during water stress in Walnut. *Plant Physiology* **128,** 282–290.

Cochard H, Nardini A, Coll L. 2004. Hydraulic architecture of leaf blades: where is the main resistance? *Plant, Cell and Environment* **27,** 1257–1267.

Cochard H, Venisse J-S, Barigah TS, Brunel N, Harbette S, Duilliot A, Tyree MT, Sakr S. 2007. Putative role of aquaporins in variable hydraulic conductance of leaves in response to light. *Plant Phyisology* **143,** 122–133.

Cowan IR. 1977. Stomatal behaviour and environment. *Advances in Botanical Research* **4,** 117–227.

Cure JD, Acock B. 1986. Crop responses to carbon dioxide doubling: A literature survey. *Agricultural and Forest Meteorology* **38,** 127–145.

Franks PJ. 2004. Stomatal control and hydraulic conductance, with special reference to tall trees. *Tree Physiology* **24,** 865–878.

Franks PJ. 2006. Higher rates of leaf gas exchange are associated with higher leaf hydrodynamic pressure gradients. *Plant, Cell and Environment* **29,** 584–592.

Franks PJ, Beerling DJ. 2009. Maximum leaf conductance driven by CO2 effects on stomatal size and density over geologic time. *Proceedings of the National Academy of Sciences, USA* **106,** 10343–10347.

Franks PJ, Drake PL, Froend RH. 2007. Anisohydric but isohydrodynamic: seasonally constant plant water potential gradient explained by a stomatal control mechanism incorporating variable plant hydraulic conductance. *Plant, Cell and Environment* **30,** 19–30.

Franks PJ, Farquhar GD. 1999. A relationship between humidity response, growth form and photosynthetic operating point in C_3 plants. *Plant, Cell and Environment* **22,** 94–100.

Franks PJ, Leitch IJ, Ruszala EM, Hetherington AM, Beerling DJ. 2012. Physiological framework for adaptation of stomata to CO_2 from glacial to future concentrations. *Philosophical Transactions of the Royal Society B–Biological Sciences* **367,** 537–546.

Guyot G, Scoffoni C, Sack L. 2011. Combined impacts of irradiance and dehydration on leaf hydraulic conductance: insights into vulnerability and stomatal control. *Plant, Cell and Environment* **35,** 857–871.

Hölttä T, Vesala T, Sevanto S, Perämäki M, Nikinmaa E. 2006. Modeling xylem and phloem water flows in trees according to cohesion theory and Münch hypothesis. *Trees–Structure and Function* **20,** 67–78.

Hölttä T, Mencuccini M, Nikinmaa E. 2009. Linking phloem function to structure: analysis with a coupled xylem–phloem transport model. *Journal of Theoretical Biology* **259,** 325–337.

Johansson I, Larsson C, Ek, B and Kjelibom. 1996. The major integral proteins of spinach leaf plasma membranes are putative aquaporins and are phosphorylated in response to Ca^{2+} apoplastic water potential. *The Plant Cell* **8,** 1181–1191.

Johnson DM, McCulloh KA, Woodruff DR, Meinzer FC. 2012. Evidence for xylem embolism as a primary factor in dehydration-induced declines in leaf hydraulic conductance. *Plant, Cell and Environment* **35,** 760–769.

Johnson DM, Meinzer FC, Woodruff DR, McCulloh KA. 2009. Leaf xylem embolism, detected acoustically and by cryo-SEM, corresponds to decreases in leaf hydraulic conductance in four evergreen species. *Plant, Cell and Environment* **32,** 828–836.

Kikuta SB, Lo Gullo MA, Nardini A, Richter H, Salleo S. 1997. Ultrasound acoustic emissions from dehydrating leaves of deciduous and evergreen trees. *Plant, Cell and Environment* **20,** 1381–1390.

Kim YX, Steudle E. 2007. Light and turgor affect the water permeability (aquaporins) of parenchyma cells in the midrib of leaves of *Zea mays*. *Journal of Experimental Botany* **58,** 4119–4129.

Lawlor DW. 2002. Limitation to photosynthesis in water-stressed leaves: stomatal vs. metabolism and the role of ATP. *Annals of Botany* **89,** 871–885.

Lawlor DW, Cornic G. 2002. Photosynthetic carbon assimilation and associated metabolism in realtin to water deficits in higher plants. *Plant, Cell and Environment* **25,** 275–294.

Locke AM, Sack L, Bernacchi CJ, Ort DR. 2013. Soybean leaf hydraulic conductance does not acclimate to growth at elevated [CO_2] or temperature in growth chambers or in the field. *Annals of Botany* **112,** 911–918.

Lo Gullo MA, Nardini A, Trifilò P, Salleo S. 2005. Diurnal and seasonal variations in leaf hydraulic conductance in evergreen and deciduous trees. *Tree Physiology* **25,** 505–512.

Maherali H, DeLucia EH, Sipe TW. 1997. Hydraulic adjustment of maple saplings to canopy gap formation. *Oecologia* **112,** 472–480.

Martorell S, Diaz-Espejo A, Medrano H, Ball MC, Choat B. 2014. Rapid hydraulic recovery in *Eucalyptus pauciflora* after drought: linkages between stem hydraulics and leaf gas exchange. *Plant, Cell and Environment* **37,** 617 – 626.

Matzner S, Comstock J. 2001. The temperature dependence of shoot hydraulic resistance: implications for stomatal behavior and hydraulic limitation. *Plant, Cell and Environment* **24,** 1299–1307.

Meinzer FC, Goldstein G, Jackson P, Holbrook NM, Guitérrez MV, Cavelier J. 1995. Environmental and physiological regulation of transpiration in tropical forest gap species: the influence of boundary layer and hydraulic properties. *Oecologia* **101,** 514–522.

Meinzer FC, Grantz DA. 1990. Stomatal and hydraulic conductance in growing sugar cane: stomatal adjustment to water transport capacity. *Plant, Cell and Environment* **13,** 383–388.

Meinzer FC, Grantz DA. 1991. Coordination of stomatal, hydraulic, and canopy boundary layer properties: Do stomata balance conductances by measuring transpiration? *Physiologia Plantarum* **83,** 324–329.

Mencuccini M. 2003. The ecological significance of long-distance water transport: short-term regulation, long-term acclimation and the hydraulic costs of stature across plant life forms. *Plant, Cell and Envrionment* **26,** 163–182.

Mencuccini M, Comstock J. 1999. Variability in hydraulic architecture and gas exchange of common bean (*Phaseolus vulgarism*) cultivars under well-watered conditions: interactions with leaf size. *Australian Journal of Plant Physiology* **26,** 115–124.

Morillon R, Chrispeels MJ. 2001. The role of ABA and the transpiration stream in the regulation of the osmotic water permeability of leaf cells. *Proceedings of the National Academy of Sciences, USA* **98,** 14138–14143.

Morison JIL, Gifford RM. 1983. Stomatal sensitivity to carbon dioxide and humidity a comparison of two C_3 and C_4 grass species. *Plant Physiology* **71,** 789–796.

Morison JIL, Lawlor DW. 1999. Interactions between increasing CO_2 concentration and temperature on plant growth. *Plant, Cell and Environment* **32,** 659–682.

Nardini A, Gortan E, Salleo S. 2005a. Hydraulic efficiency of the leaf venation system in sun- and shade-adapted species. *Functional Plant Biology* **32,** 953–961.

Nardini A, Salleo S, Andri S. 2005b. Circadian regulation of leaf hydraulic conductance in sunflower (*Helianthus annuus* L. cv Margot). *Plant, Cell and Environment* **28,** 750–759.

Nardini A, Salleo S, Jansen S. 2011. More than just a vulnerable pipeline: xylem physiology in the light of ion-mediated regulation of plant water transport. *Journal of Experimental Botany* **62,** 4701–4718.

Nikinmaa E, Hölttä T, Hari P, Kolari P, Mäkelä A, Sevanto, S, Vesala T. 2013. Assimilate transport in phloem sets conditions for leaf gas exchange. *Plant, Cell and Environment* **36,** 655–669.

Oren R, Sperry JS, Katul GG, Pataki DE, Ewers BE, Phillips N, Schäfer KVR. 1999. Survey and synthesis of intra- and interspecific variation in stomatal sensitivity to vapour pressure deficit. *Plant, Cell and Environment* **22,** 1515–1526.

Pantin F, Monner F, Jannoud D, Costa J M, Renaud J, Muller B, Simonneau T, Genty B. 2012. The dual effect of abscisic acid on stomata. *New Phytologist* **197,** 65–72.

Peak D, Mott KA. 2011. A new, vapour-phase mechanism for stomatal responses to humidity and temperature. *Plant, Cell and Environment* **34,** 162–178

Pieruschka R, Huber G, Berry JA 2010. Control of transpiration by radiation. *Proceedings of the National Academy of Sciences, USA* **107,** 13372–13377.

Pou A, Medrano H, Flexas J, Tyerman S. 2013. A putative role for TIP and PIP aquaporins in dynamics of leaf hydraulic and stomatal conductances in grapevine under water stress and re-watering. *Plant, Cell and Environment* **36,** 828–843.

Quinn JF, Dunham AE. 1983. On hypothesis testing in ecology and evolution. *The American Naturalist* **122,** 602–617.

Rockwell F, Holbrook NM, Stroock AD. 2014. The competition between liquid and vapor transport in transpiring leaves. *Plant Physiology* doi: 10.1104/pp.114.236323.

Sack L, Holbrook NM. 2006. Leaf hydraulics. *Annual Review of Plant Biology* **57,** 361–381.

Sack L, Scoffoni C. 2013. Leaf venation: structure, function, development, evolution, ecology and applications in the past, present and future. *New Phytologist* **198,** 983–1000.

Sack L, Streeter CM, Holbrook NM. 2004. Hydraulic analysis of water flow through leaves of sugar maple and red oak. *Plant Physiology* **134,** 1824–1833.

Sack L, Tyree MT, Holbrook NM. 2005. Leaf hydraulic architecture correlates with regeneration irradiance in tropical rainforest trees. *New Phytologist* **167,** 403–413.

Salleo S, Lo Gullo MA, Raimondo F, Nardini A. 2001. Vulnerability to cavitation of leaf minor veins: any impact on leaf gas exchange? *Plant, Cell and Environment* **24,** 851–859.

Scoffoni C, Pou A, Aasamaa K, Sack L. 2008. The rapid light response of leaf hydraulic conductance: new evidence from two experimental methods. *Plant, Cell and Environment* **31,** 1803–1812.

Sellin A, Kupper P. 2005a. Within-crown variation in leaf conductance of Norway spruce: effects of irradiance, vapour pressure deficit, leaf water status and plant hydraulic constraints. *Annals of Forest Science* : **61,** 419–429.

Sellin A, Kupper P. 2005b. Variation in leaf conductance of silver birch: effects of irradiance, vapour pressure deficit, leaf water status and position within a crown. *Forest Ecology and Management* **206,** 153–166.

Sellin A, Kupper P. 2007. Temperature, light and leaf hydraulic conductance of little-leaf linden (*Tilia cordata*) in a mixed forest canopy. *Tree Physiology* **27,** 679–688.

Sellin A, Õunapuu E, Kupper P. 2008. Effects of light intensity and duration on leaf hydraulic conductance and distribution of resistance in shoots of silver birch (*Betula pendula*). *Physiologia Plantarum* **134,** 412–420.

Shatil-Cohen A, Attia Z, Moshelion M. 2011. Bundle-sheath cell regulation of xylem–mesophyll water transport via qauaporins under drought stress: a target of xylem-borne ABA? *The Plant Journal* **67,** 72–80.

Simonin KA, Limm EB, Dawson TE. 2012. Hydraulic conductance of leaves correlates with leaf lifespan: implications for lifetime carbon gain. *New Phytologist* **193,** 939–947.

Sôber A. 1997. Hydraulic conductance, stomatal conductance, and maximal phosotynthetic rate in bean leaves. *Photosynthetica* **34,** 599–603.

Sperry JS. 2000. Hydraulic constraints on plant gas exchange. *Agricultural and Forest Meteorology* **104,** 13–23.

Sperry JS, Pockman WT. 1993. Limitation of transpiration by hydraulic conductance and xylem cavitation in *Betula occidentalis*. *Plant, Cell and Environment* **16,** 279–287.

Sperry JS, Hacke UG, Oren R, Comstock JP. 2002. Water deficits and hydraulic limits to leaf water supply. *Plant, Cell and Environment* **25,** 251–263.

Thompson MV, Holbrook NM. 2004. Scaling phloem transport: information transmission. *Plant, Cell and Environment* **27,** 509–519.

Tolley LC, Strain BR. 1985. Effects of CO_2 enrichment and water stress on gas exchange of *Liquidambar styraciflua* and *Pinus taeda* seedlings grown under different irradiance levels. *Oecologia* **65,** 166–172.

Turgeon R. 2010. The puzzle of phloem pressure. *Plant Physiology* **154,** 578–581.

Tyree MT, Cheung YNS. 1977. Resistance to water flow in *Fagus grandifolia* leaves. *Canadian Journal of Botany* **55,** 2591–2599.

Tyree MT, Cruiziat P, Benis M LoGullo MA, Salleo S. 1981. The kinetics of rehydration of detached sunflower leaves from different initial water deficits. *Plant, Cell and Environment* **4,** 309–317.

Winkel T, Rambal S. 1993. Influence of water stress on grapevines growing in the field: from leaf to whole-plant response. *Australian Journal of Plant Physiology* **20,** 143–157.

Zwieniecki MA, Brodribb TJ, Holbrook NM. 2007. Hydarulic design of leaves: insights from rehydration kinetics. *Plant, Cell and Environment* **30,** 910–921.

Zwieniecki MA, Melcher PJ, Holbrook NM. 2001. Hydrogel control of xylem hydraulic resistance in plants. *Science* **291,** 1059–1062.